Mon. Not. R. Astron. Soc. **000**, 000–000 (0000) Printed 2 February 2008 (MN LaTeX style file v2.2)

Discovery of new 19.9-GHz methanol masers in star forming regions

S.P. Ellingsen[1], D.M. Cragg[2], J.E.J. Lovell[3], A.M. Sobolev[4],
P.D. Ramsdale[1], P.D. Godfrey[2]
[1] *School of Mathematics and Physics, University of Tasmania, Private Bag 21, Hobart, Tasmania 7001, Australia;*
Simon.Ellingsen@utas.edu.au
[2] *School of Chemistry, Building 23, Monash University, Victoria 3800, Australia;*
Dinah.Cragg@sci.monash.edu.au, Peter.Godfrey@sci.monash.edu.au
[3] *Australia Telescope National Facility, CSIRO, PO Box 76, Epping, NSW 2121, Australia;*
Jim.Lovell@csiro.au
[4] *Astronomical Observatory, Ural State University, Lenin Street 51, Ekaterinburg 620083, Russia;*
Andrej.Sobolev@usu.ru

arXiv:astro-ph/0407246v1 13 Jul 2004

2 February 2008

ABSTRACT

We have used the NASA Tidbinbilla 70-m antenna to search for emission from the 2_1-3_0 E (19.9-GHz) transition of methanol. The search was targeted towards 22 star formation regions which exhibit maser emission in the 107.0-GHz 3_1-4_0 A$^+$ methanol transition, as well as in the 6.6-GHz 5_1-6_0 A$^+$ transition characteristic of class II methanol maser sources. A total of 7 sources were detected in the 2_1-3_0 E transition, 6 of these being new detections. Many of the new detections are weak ($\lesssim 0.5$ Jy), however, they appear to be weak masers rather than thermal or quasi-thermal emission.

We find a strong correlation between sources which exhibit 19.9-GHz methanol masers and those which both have the class II methanol masers projected against radio continuum emission and have associated 6035-MHz OH masers. This suggests that the 19.9-GHz methanol masers arise in very specific physical conditions, probably associated with a particular evolutionary phase. In the model of Cragg, Sobolev & Godfrey (2002) these observations are consistent with gas temperatures of 50 K, dust temperatures of 150-200 K and gas densities of $10^{6.5} - 10^{7.5}$ cm^{-3}.

Key words: masers – stars:formation – ISM: molecules – radio lines : ISM

1 INTRODUCTION

In the 20 years since the discovery of the first of the class II methanol maser transitions (Wilson et al. 1984) they have become important probes of high-mass star formation regions. Class II methanol masers have a number of advantages over the other molecular maser species commonly found in star forming regions. They are more common than main-line OH masers and where they are found towards the same regions they are typically an order of magnitude stronger (Caswell et al. 1995a). They are significantly less variable than 22-GHz water masers, with individual features having lifetimes in excess of a decade and unlike OH and water masers they appear to be exclusively associated with high-mass star formation (Minier et al. 2003).

To date more than 20 different methanol transitions have been observed as interstellar masers, and these have been empirically divided into two classes (Menten 1991a). Class II methanol masers are closely associated with high-mass star formation and other tracers of this process, far-infrared sources, HII regions and OH and water masers. Class I masers are also found within high-mass star forming regions, but offset from the young stellar objects and are thought to be collisionally pumped in outflows. The most common class II methanol maser transitions are those at 6.6 and 12.1 GHz (Menten 1991b; Batrla et al. 1987), but some sources such as W3(OH), NGC6334F and 345.010+1.792 exhibit methanol maser emission from many other transitions (Cragg et al. 2001; Sutton et al. 2001). Interferometric observations have shown that the 6.6- and 12.1-GHz emission in some sources is coincident both in velocity and spatially (to within a few milliarcseconds) (Menten et al. 1992; Norris et al. 1993; Minier, Booth & Conway 2000). Observations with arcsecond resolution of some of the rarer transitions in W3(OH) show that to within the relative positional accuracy these are also spatially coincident with the 6.6-GHz masers (Menten et al. 1988; Sutton et al. 2001).

The pumping of interstellar masers is a complicated process that sensitively depends upon a number of factors such as the gas temperature and density, molecular abundance and external radiation field. Theoretical studies of maser pumping show that the commonly observed maser transitions are produced over a wide range of physical conditions (Cragg et al. 2002; Gray, Field & Doel 1992; Pavlakis & Kylafis 1996a,b; Sobolev et al. 1997) and hence it isn't possible to infer any detailed information about the physical conditions in the maser region from observations of a single transition. However, where multiple transitions arise from the same gas any maser pumping scheme must be able to simultaneously produce the various transitions in the observed intensity ratio. This approach has been applied to OH and methanol maser emission in a small number of sources and produces physically plausible answers (Cesaroni & Walmsley 1991; Cragg et al. 2001; Sutton et al. 2001). Typically the star-forming regions targetted in searches for new maser transitions and multi-transition modelling are those which exhibit emission from a large number of maser transitions such as W3(OH) and NGC6334F. However, the presence of a large number of different maser transitions in these sources indicates that these regions are special in some way, and not representative of the conditions that exist in the majority of high-mass star forming regions. In order to obtain information on the conditions in a larger sample of more representative star forming regions we are undertaking a program to search for methanol maser transitions that are rarely strong, (hence forth referred to as "weak methanol" maser transitions for simplicity) towards all sources that exhibit 107.0-GHz methanol maser emission. To date 25 such sources have been identified from searches of more than 175 class II methanol maser sources (Val'tts et al. 1995, 1999; Caswell et al. 2000; Minier & Booth 2002). In constraining the physical conditions in these regions the non-detection of the weak methanol maser transitions can sometimes be as useful as a detection, as it also limits the range of parameter space within the model consistent with observations of the region (see for example Cragg et al. 2004).

We have previously undertaken searches for 23.1-, 85.5-, 86.6- and 108.8-GHz methanol masers towards the sample of star formation regions with 107.0-GHz methanol masers (Cragg et al. 2004; Ellingsen et al. 2003; Val'tts et al. 1999). Although it was one of the first methanol maser transitions discovered, few observations have been made of the 19.9-GHz 2_1-3_0 E transition and it has only been reported towards three star forming regions, W3(OH), NGC7538 (Wilson et al. 1985) and NGC6334F (Menten & Batrla 1989). Here we report the results of a sensitive search for maser emission from the 2_1-3_0 E transition of methanol with the Tidbinbilla 70-m antenna. The search was targetted towards the 22 known 107.0-GHz methanol maser sources that are observable from Tidbinbilla.

2 OBSERVATIONS AND DATA REDUCTION

The observations of the 19.9-GHz 2_1-3_0 E transition were made on 2003 April 10, October 25 & 26 and November 15-17 using the NASA Tidbinbilla 70-m antenna. The rest frequency assumed was 19967.3961 MHz, which has a 2σ uncertainty of 0.0002 MHz (Mehrotra, Dreizler & Mäder 1985). At 19.9 GHz the FWHM antenna beamwidth was $53''$. The sources were observed in position switching mode with 300 seconds spent at the onsource position and 150 seconds spent at a position offset by +2.5 minutes in right ascension prior to the onsource observation and another 150 seconds spent at a position offset by -2.5 minutes in right ascension following the observation. This observing pattern means that the movement of the antenna during the observation is the same for both the onsource and reference observations and minimises the difference in atmospheric and antenna gain effects between them. The weather conditions varied considerably during the observations and the majority of the sources were observed on more than one occasion. The observations made in good weather conditions typically have a sensitivity a factor of two or more better than those observed in poor conditions. For sources observed in good weather conditions an onsource integration time of 5 minutes typically yielded an RMS of 0.1 Jy. The data for a single circular polarization (LCP) were collected using a 2-bit, three level digital autocorrelation spectrometer configured with 4096 channels spanning a 16-MHz bandwidth. For an observing frequency of 19.9 GHz this configuration produces a natural weighting velocity resolution of 0.07 km s^{-1}, or 0.12 km s^{-1} after Hanning smoothing. The total velocity range covered was approximately 240 km s^{-1}, and for each source this centred around the velocity of the 6.6-GHz methanol maser emission. Tipping curves to measure the opacity of the atmosphere were performed for the observations made in November. For the earlier observations the opacity was estimated either from the variation in the system temperature with elevation, or from tipping scans made at other frequencies. The nominal pointing accuracy of the Tidbinbilla 70-m antenna is $10''$ and comparison of sources observed on more than one occasion suggests that the final absolute flux density calibration is accurate to 10%

For some of the sources detected at 19.9 GHz, additional observations at 6.6 and 12.1 GHz were made with the University of Tasmania 26-m antenna at Hobart on 2003 December 1 & 2. At 6.6- and 12.1-GHz the FWHM beamwidths were $7.1'$ and $3.9'$ respectively. At both frequencies the observations were made with a dual circularly polarized receiver with a typical system equivalent flux density of 880 Jy at 6.6 GHz and 790 Jy at 12.1 GHz. The data were collected using a 2-bit, three level digital autocorrelation spectrometer configured with 4096 channels spanning a 4-MHz bandwidth at 6.6 GHz and 2048 channels spanning an 8-MHz bandwidth at 12.1 GHz. This configuration produces a natural weighting velocity resolution of 0.05 km s^{-1}, or 0.09 km s^{-1} after Hanning smoothing at 6.6 GHz, and natural weighting and Hanning smoothed velocity resolutions of 0.12 and 0.19 km s^{-1} at 12.1 GHz. This velocity resolution is well matched to that of the 19.9-GHz observations. The sources were observed in position switching mode with 600 seconds spent at a position offset in position by -1 degree in declination and 600 seconds spent onsource at 6.6 GHz and 60 seconds spent onsource at 12.1 GHz. In addition a five point grid with observations at the nominal position and at four points each offset by approximately half the FWHM beamwidth were made for each source at both fre-

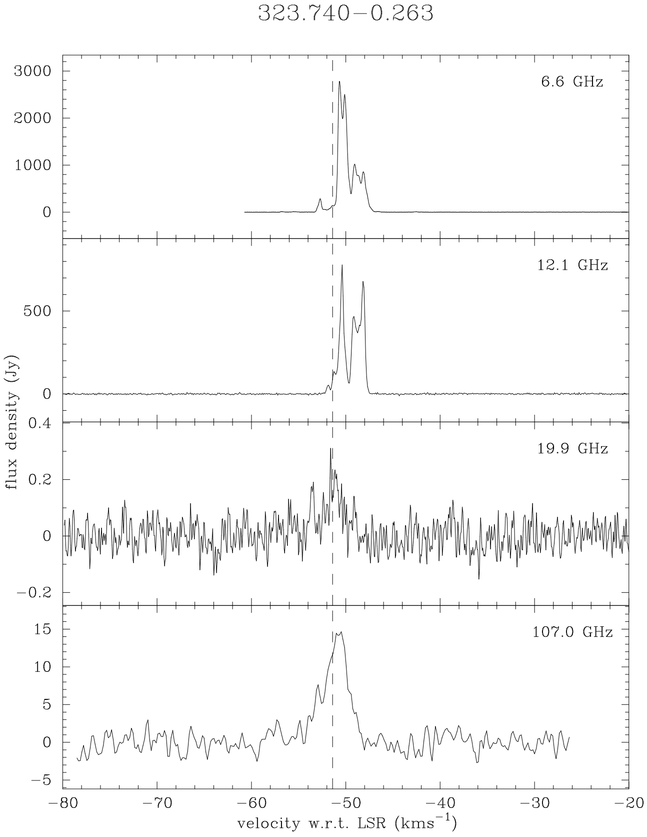

Figure 2. 6.6-, 12.2-, 19.9- and 107.0-GHz methanol emission towards 323.740-0.263. The 107.0-GHz spectrum is from Val'tts et al. (1999).

quencies. These data were used to measure any pointing offset and the flux density of each source has been scaled to correct for the offset. Analysis of the grid observations revealed that the 12.1 GHz observations were made with the receiver significantly offset from the optimal position. The absolute flux density calibration of the 6.6-GHz observations is better than 10%, however, uncertainties due to the offset receiver position mean that at 12.1 GHz the calibration is probably only good to a factor of 2.

3 RESULTS

A total of 22 sources were observed at 19.9 GHz and these are listed in Table 1. Emission from the 19.9-GHz 2_1-3_0 E transition was detected towards 7 sources, all of these except NGC6334F are new discoveries. The 19.9-GHz spectrum of each of the detected sources is shown in Fig. 1. For the sources where emission was detected Gaussian profiles were fitted and the parameters of these are listed in Table 1, for the other sources a limit of three times the RMS noise in the final spectra is given. The typical 3-σ limit for these observations was less than 0.3 Jy which is significantly better than our searches for the 23.1-, 85.5-, 86.6- and 108.8-GHz transitions. Of the 7 sources detected only two have a peak flux density stronger than 1 Jy and so these observations demonstrate the importance of sensitivity in searches for weak methanol maser transitions. The weakness of the 19.9-GHz methanol emission in most of our detections means that we cannot conclusively prove that it is maser emisison, however, comparison with other methanol maser transitions in each source shown in Figs 2-8 strongly suggests that for the majority it is. The recent upgrade to the Australia Telescope Compact Array (ATCA) means that it is now able to observe the 19.9-GHz methanol transition and hence will be able to determine whether the weak sources are masers.

3.1 Comments on individual sources

323.740-0.263

This is one of the strongest 6.6- and 12.1-GHz methanol masers, however at 19.9 GHz it was only marginally detected with a peak flux density of 0.15 Jy and a FWHM of 3.1 km s^{-1}. The velocity and width of the 19.9-GHz emission is similar to that seen at both 107.0- and 156.6-GHz (Caswell et al. 2000). Caswell et al. interpret the strong 107.0-GHz emission as being due to a blend of maser lines, with some thermal contribution and the 156.6-GHz emission as being thermal. Fig. 2 shows that the 19.9-GHz emission appears to be slightly offset from the strongest 6.6- and 12.1-GHz masers, although the low signal-to-noise ratio means that it is not possible to be definitive about this. The weak, broad nature of the 19.9-GHz emission in this source and its alignment with thermal emission from other methanol transitions (Caswell et al. 2000) means that it may too be thermal, but higher spatial resolution observations are required to determine this.

323.740-0.263 is an unusual star forming region in that although it shows extremely strong class II methanol maser emission Phillips et al. (1998) did not detect centimetre radio continuum emission with a 4-σ limit of 0.2 mJy/beam. Infra-red emission is present towards 323.740-0.263, but only at wavelengths in excess of 3.6 μm (De Buizer, Piña & Telesco 2000; Walsh, Lee & Burton 2002). From their 10 and 18 μm observations De Buizer et al. calculate a dust temperature of 128 K. Walsh et al. also detected H_2 emission from the region surrounding the masers, some of which appears to be shocked excited.

328.808+0.633

Fig. 3 shows that the 19.9-GHz methanol maser emission in this source has the same peak velocity as the weak 85.5-GHz emission detected by Ellingsen et al. (2003), which is slightly offset in velocity from the strongest 6.6- and 107.0-GHz emission. The 12.2-GHz emission at velocities near -44 km s^{-1} is not detected in our Mt Pleasant observations, but Caswell et al. (1995b) found emission with a strength of 1-2 Jy in this velocity range (beneath the detection threshold of the Mt Pleasant observations). The emission at 107.0-GHz has both maser and thermal components, while the emission at 108.8- and 156.6-GHz is thought to be thermal (Caswell et al. 2000; Val'tts et al. 1999), and is offset from the velocity of the 19.9-GHz methanol maser emission.

The class II methanol masers in 328.808+0.633 are projected against a strong cometary HII region (Walsh et al. 1998) and 1720-, 4765-, 6030- and 6035-MHz OH masers have all been detected within a few arcseconds of the

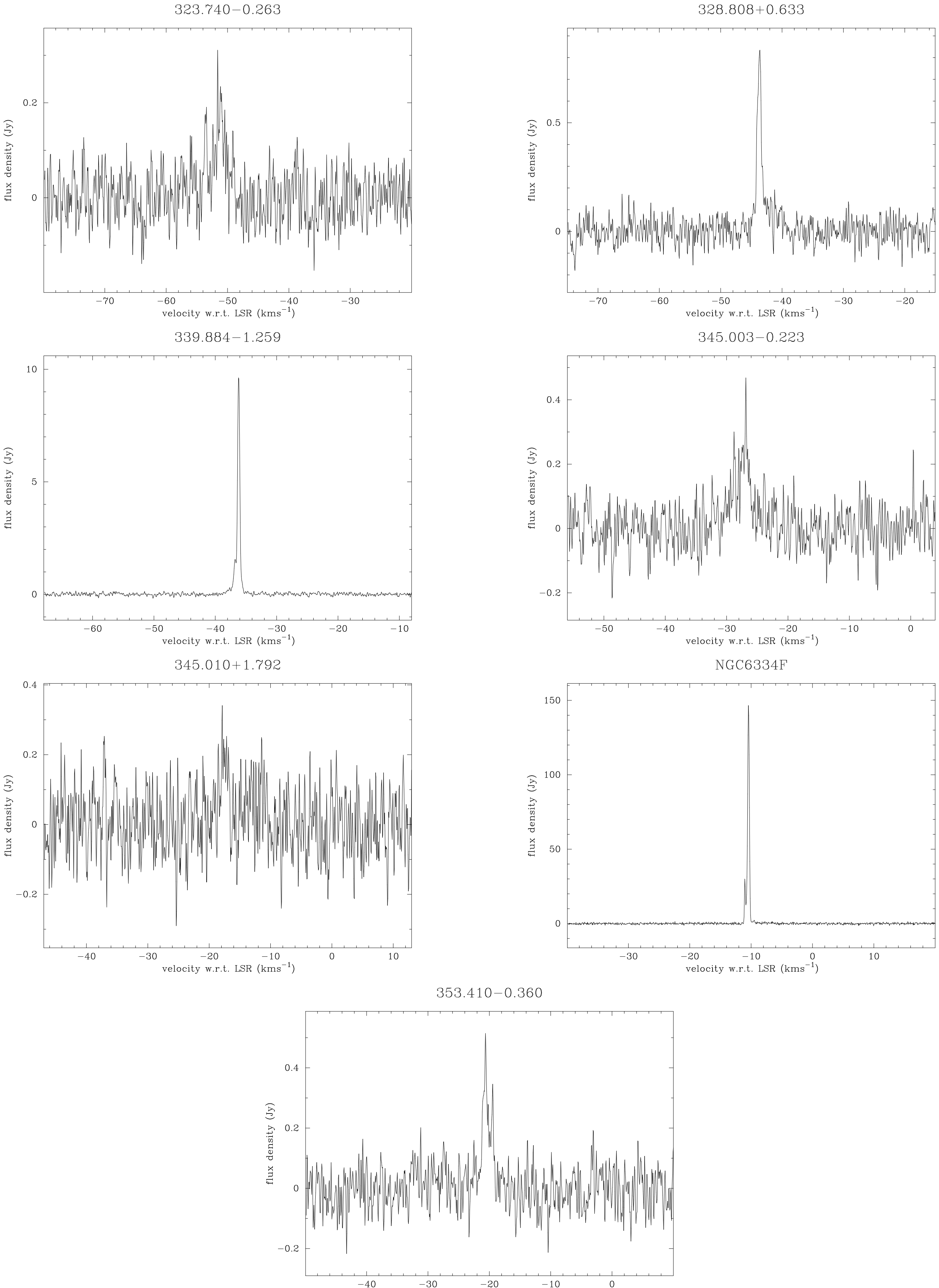
323.740−0.263

328.808+0.633

339.884−1.259

345.003−0.223

345.010+1.792

NGC6334F

353.410−0.360

Table 1. A list of sources observed at 19.9-GHz. For sources where emission was detected the values listed are those of Gaussian profiles fitted to the spectra. For sources where no emission was detected the value listed is 3 x the RMS noise level in the Hanning smoothed spectrum. DOY 100 = 10 April 2003 ; DOY 299 = 26 October 2003 ; DOY 319 = 15 November 2003

Name	**R.A.(J2000) (h m s)**	**Dec.(J2000) (° ′ ″)**	**Observed DOY 2003**	**Integration Time (min)**	**Flux Density (Jy)**	**Velocity (km s^{-1})**	**FWHM (km s^{-1})**
188.946+0.886	06:08:53.3	+21:38:29	100	10	<0.20		
192.600–0.048	06:12:54.0	+17:59:24	100	10	<0.19		
310.144+0.760	13:51:58.5	–61:15:42	300,320	10	<0.16		
318.948–0.196	15:00:55.4	–58:58:53	300,320	10	<0.17		
323.740–0.263	15:31:45.5	–56:30:50	299,319	10	0.15	-51.4	3.1
327.120+0.511	15:47:32.7	–53:52:38	300,320	10	<0.17		
328.808+0.633	15:55:48.5	–52:43:07	300,319,320	15	0.79	-43.7	0.9
336.018–0.827	16:35:09.3	–48:46:47	320	5	<0.21		
339.884–1.259	16:52:04.7	–46:08:34	299,319,320	15	9.8	-36.2	0.4
					1.5	-36.8	0.4
340.054–0.244	16:48:13.9	–45:21:44	320	5	<0.20		
340.785–0.096	16:50:14.8	–44:42:26	320	5	<0.76		
345.003–0.223	17:05:10.9	–41:29:06	321	5	0.22	-27.4	3.4
345.010+1.792	16:56:47.6	–40:14:26	320	5	0.21	-17.6	1.5
345.504+0.348	17:04:22.9	–40:44:22	300	5	<0.65		
348.703–1.043	17:20:04.1	–38:58:31	320	5	<0.39		
NGC6334F	17:20:53.4	–35:47:01	320	5	146.7	-10.4	0.3
					26.8	-11.0	0.3
					1.9	-9.6	0.4
353.410–0.360	17:30:26.2	–34:41:46	320,321	7	0.33	-20.5	1.8
9.621+0.196	18:06:14.7	–20:31:32	320,321	12	<0.22		
12.909–0.260	18:14:39.5	–17:52:00	320	10	<0.27		
23.010–0.411	18:34:40.3	–09:00:38	320	10	<0.26		
23.440–0.182	18:34:39.2	–08:31:24	320	10	<0.24		
35.201–1.736	19:01:45.5	+01:13:35	320	10	<0.51		

methanol masers (Caswell 2003, 2004; Dodson & Ellingsen 2002). The masers are also associated with a mid-infrared source, from which a dust temperature of approximately 120 K is inferred (De Buizer et al. 2000).

339.884-1.259

The strong, narrow emission at 19.9 GHz in this source identifies it unambiguously as maser emission. The 19.9-GHz methanol masers are at velocities in the middle of the range seen in the 6.6- and 12.1-GHz masers. Fig. 4 shows that the strongest 19.9-GHz methanol maser emission in 339.884-1.259 is at a velocity corresponding to one of the weaker peaks in the 12.1- and 107.0-GHz emission. The observations of Caswell et al. (1995a) show that at the corresponding velocity the 6.6-GHz is at a minimum. Very long baseline interferometry observations by Phillips (1998) show a narrow 6.6-GHz emission feature with a flux density of approximately 300 Jy at a velocity of -36.1 km s^{-1}. The observations of Caswell et al. (2000) suggest that both the 107.0 and weaker 156.6-GHz methanol masers are superimposed on top of thermal emission and show significant variations on a timescale of years.

The class II methanol masers in this source are projected against the centre of a weak cometary HII region (Ellingsen, Norris & McCulloch 1996) and 1720-, 6030- and 6035-MHz OH masers have all been detected within a few arcseconds of the methanol masers (Caswell 2003, 2004). De Buizer et al. (2002) detect three mid infra-red sources close to the masers with a peak dust temperature of 145 K and suggest that some of the radio continuum emission results from a collimated ionized outflow.

345.003-0.223

The 19.9-GHz methanol masers in 345.003-0.223 follow the pattern of the majority of the other sources in being offset in velocity from the strongest emission at 6.6-GHz (see Fig. 5), but coincident in velocity with a weaker emission feature. However, the peak flux densities of the 6.6-, 12.1- and 107.0-GHz masers in this source are significantly less than for the other sources (Caswell et al. 1995b, 2000). The velocity of the 19.9-GHz peak lies between the velocity of the thermal emission at 156.6-GHz (-27.8 km s^{-1}) and the peak of the 107.0-GHz maser emission (-26.9 km s^{-1}), which also lies on top of broad thermal emission (Caswell et al. 2000). The 12.1-GHz maser emission from the velocity range of the 19.9-GHz maser is very weak (of the order of 1 Jy) (Caswell et al. 1995b) and comparison of the 6.6-GHz emission shown by Caswell et al. (1995a) with that in Fig. 5 shows that the 6.6-GHz peak flux density is less than 20% of that observed a decade ago.

Walsh et al. (1998) found the 6.6-GHz methanol masers in this source to lie in two clusters, the emission near -27 km s^{-1} is projected against an HII region and 1720-, 6030- and 6035-MHz OH masers have all been detected within a few arcseconds of the class II methanol masers (Caswell 2003, 2004)

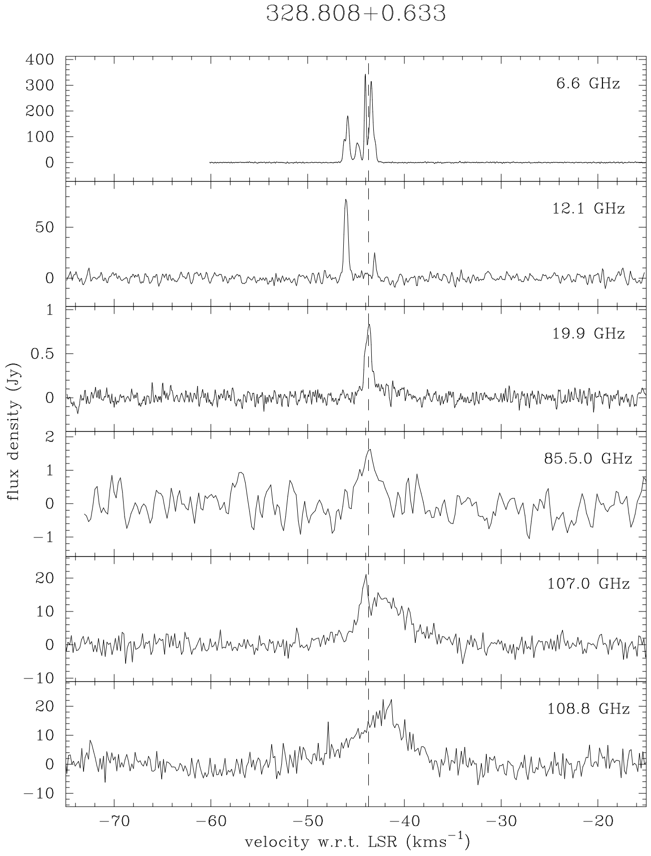

Figure 3. 6.6-, 12.2-, 19.9-, 85.5-, 107.0- and 108.8-GHz methanol emission towards 328.808+0.633. The 85.5-GHz spectrum is from Ellingsen et al. (2003) and the 107.0- and 108.8-GHz spectra are from Val'tts et al. (1999).

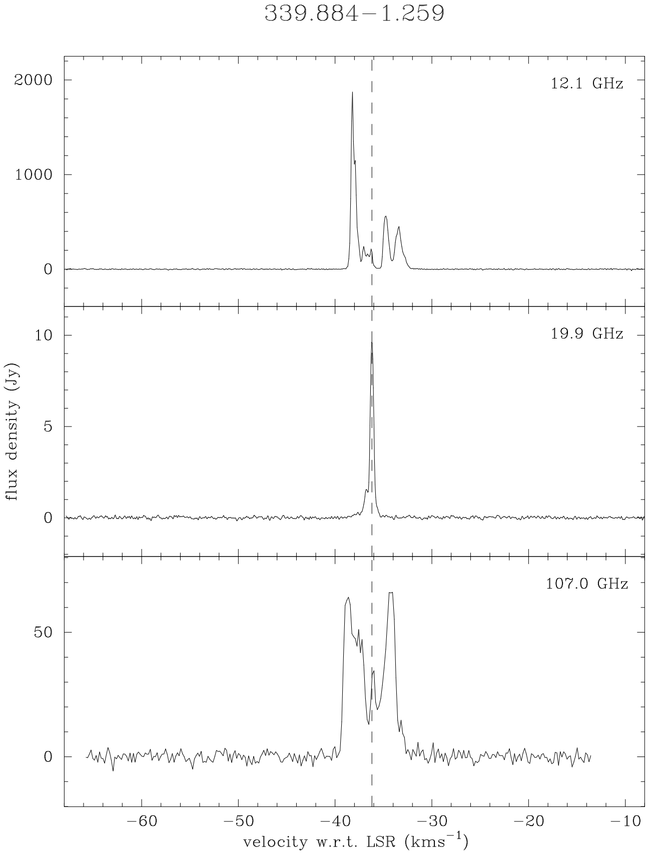

Figure 4. 12.2-, 19.9- and 107.0-GHz methanol emission towards 339.884-1.259. The 107.0-GHz spectrum is from Val'tts et al. (1999).

345.010+1.792

345.010+1.792 is a remarkable source which exhibits class II methanol maser emission in nearly every known transition in which it has been observed (Val'tts 1998; Val'tts et al. 1999; Cragg et al. 2001), to date the only exception is the 23.1-GHz transition (Cragg et al. 2004). However, as can be seen in Fig. 6 the 19.9-GHz methanol maser emission differs from the other weak methanol transitions which are generally observed at velocities near -22 km s^{-1} (Cragg et al. 2001). The 19.9-GHz maser emission at -17.6 km s^{-1} corresponds to a 100 Jy 6.6-GHz emission feature, which at one time was the strongest feature in the spectrum, but has significantly declined in strength over the last decade (Caswell et al. 1995a). There is 12.1- and 107.0-GHz emission present at the velocity of the 19.9-GHz emission, but only at a level of a few Jy (Caswell et al. 2000). Strong thermal emission (most evident in the 108.8-GHz spectrum) is also present in many of the millimetre methanol transitions that have been observed towards 345.010+1.792, however, it is well offset in velocity from the 19.9-GHz peak and the other weak methanol maser transitions.

The class II methanol masers are projected against an HII region, although significantly offset from the centre (Walsh et al. 1998). The 10 and 18 μm MIR emission associated with the masers implies a dust temperature of approximately 160 K (De Buizer et al. 2000) and 6030- and 6035-MHz OH masers are located within a few arcseconds of the methanol (Caswell 2003).

NGC6334F

NGC6334F is the archetypal high-mass star forming region of the southern sky, it shares many characteristics with W3(OH) and has been well studied over a range of wavelengths and molecular transitions. It remains the strongest known 19.9-GHz methanol maser source, although it has significantly decreased in strength over the 16 year period since its discovery (Menten & Batrla 1989). Unlike most of the other 19.9-GHz methanol maser sources Fig. 7 shows that in NGC6334F the 19.9-GHz peak is at the same velocity as the peak flux density at 6.6-, 12.1- and 107.0-GHz. There are two regions of class II methanol maser emission near NGC6334F, separated by about 6 arcseconds, one projected onto the HII region, the other offset from it (Ellingsen et al. 1996). Unfortunately both clusters show strong emission at velocities around -10.4 km s^{-1} and interferometric resolution observations are required to determine which of the clusters the 19.9-GHz emission is associated with.

NGC6334F has 1720-, 6030- and 6035-MHz OH masers within a few arcseconds of the class II methanol maser cluster projected onto a strong HII region (Caswell 2003, 2004). There are a number of MIR sources in the NGC6334F region, the strongest of which coincides with the peak of the

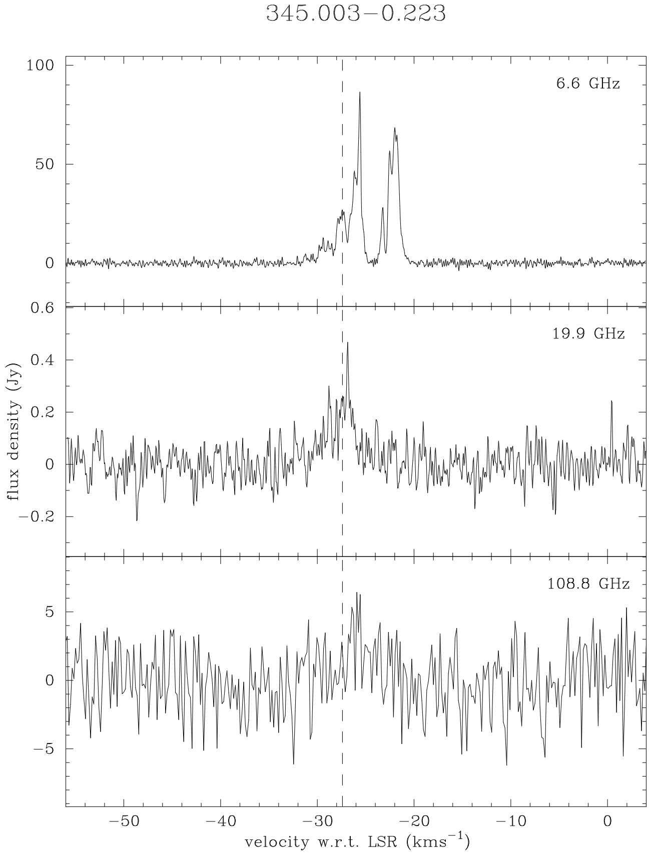

Figure 5. 6.6-, 19.9- and 108.8-GHz methanol emission towards 345.003-0.223. The 108.8-GHz spectrum is from Val'tts et al. (1999).

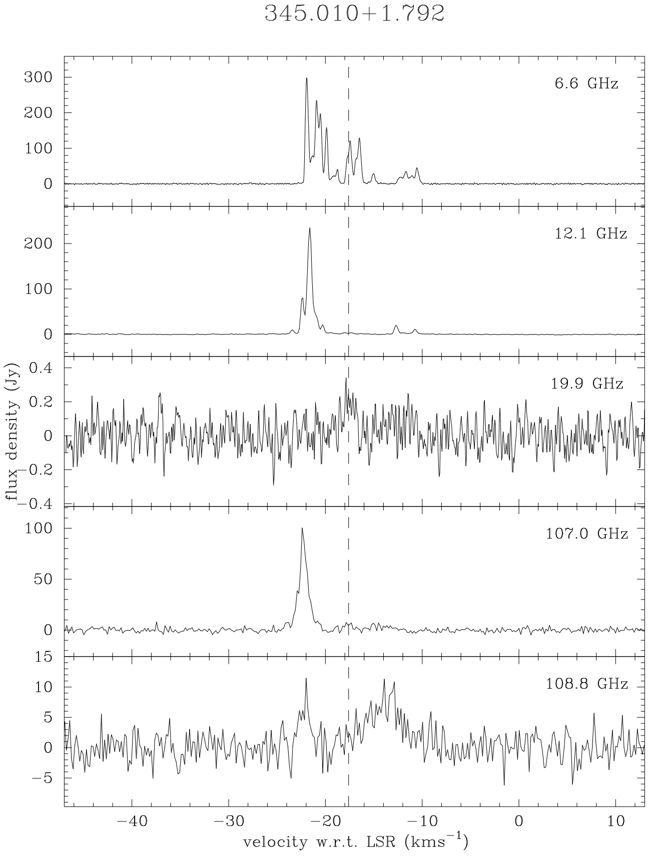

Figure 6. 6.6-, 12.2-, 19.9-, 107.0- and 108.8-GHz methanol emission towards 345.010+1.792. The 12.2-GHz spectrum is from Cragg et al. (2001) and the 107.0- and 108.8-GHz spectra are from Val'tts et al. (1999).

radio continuum and maser cluster (De Buizer et al. 2000). De Buizer et al. estimate a dust temperature of 159 K from their observations.

353.410-0.360

Fig. 8 shows that the 19.9-GHz methanol maser emission in 353.410-0.360 follows the pattern seen in most of the other sources, being aligned in velocity with secondary 6.6-GHz and 12.1-GHz peaks (Caswell et al. 1995b). The class II methanol masers are projected onto an HII region with a peak flux density of 215 mJy/beam at 3-cm (Phillips et al. 1998) and 1720-, 4765-, 6030- and 6035-MHz OH masers are located within a few arcseconds (Caswell 2003, 2004; Dodson & Ellingsen 2002).

4 DISCUSSION

Table 4 presents a nearly complete set of observations of 25 class II methanol maser sources in 9 transitions. The selected sources all exhibit masers at 6.6 and 107.0 GHz, and all but 1 also have masers detected at 12.1 GHz (although in some cases not at the velocity of the 107.0 GHz peak). Of the remaining 6 frequencies surveyed, the 19.9-GHz maser which is the subject of this paper is detected in the largest number of sources (9), followed by the 156.6-GHz maser (4 sources), the 23.1-GHz maser (3 sources), the 85.5- and 86.6-GHz masers (2 sources each), and the 108.8-GHz maser (1 source). While these statistics demonstrate that these other maser transitions are rarely strong, they suffer from a number of limitations. The searches at different frequencies were carried out with different sensitivities, some are incomplete, and the detectability of weak millimetre-wavelength masers is often compromised by overlapping thermal emission. Nevertheless, the general scarcity of the weaker masers helps delimit the conditions prevalent in our sample of 107.0-GHz maser sources, as is outlined in section 4.2.

4.1 Association with radio continuum and 6-GHz OH masers

It is clear from the comments on the individual sources that most 19.9-GHz methanol masers are :

- offset in velocity from the strongest 6.6- and 12.1-GHz masers ;
- occur in sources that are projected against centimetre continuum emission ;
- have associated 6030- and 6035-MHz OH masers.

Our observations include 7 of the 9 sources known to exhibit 19.9-GHz methanol maser emission (the other two being W3(OH) and NGC7538). Both W3(OH) and NGC7538

Landscape table to go here

Table 2.

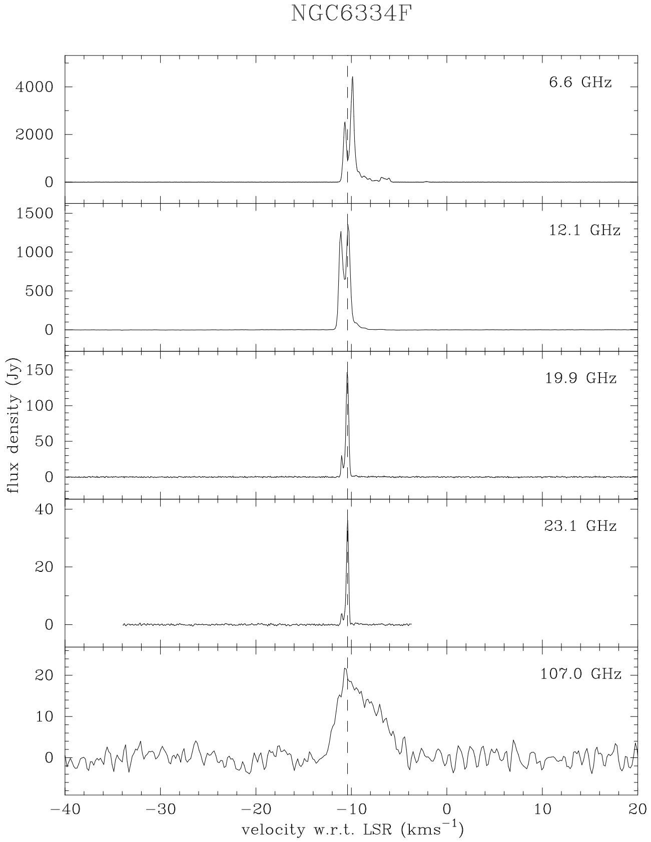

Figure 7. 6.6-, 12.2-, 19.9-, 23.1- and 107.0-GHz methanol emission towards NGC6334F. The 12.2-GHz spectrum is from Cragg et al. (2001), the 23.1-GHz spectrum is from Cragg et al. (2004) and the 107.0-GHz spectrum is from Val'tts et al. (1999).

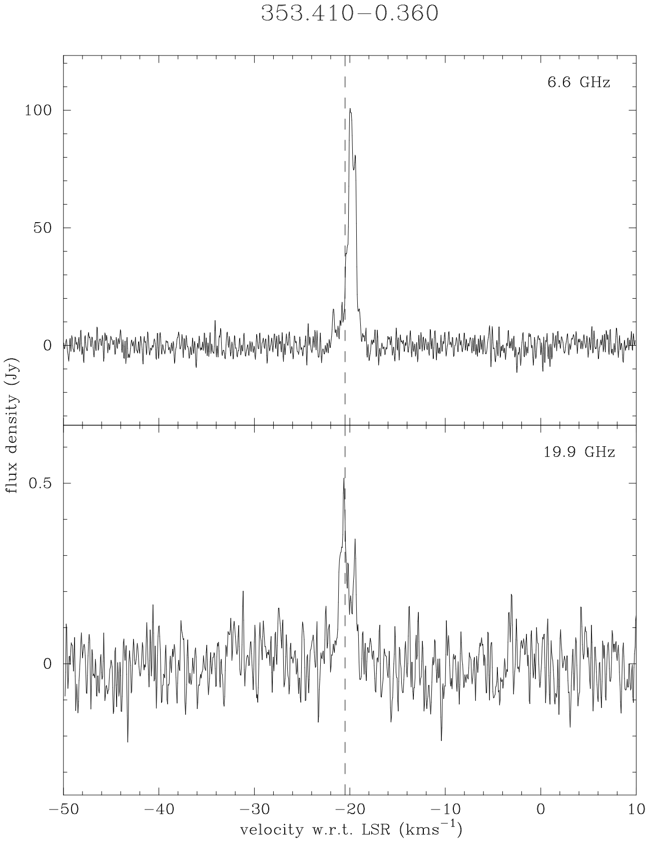

Figure 8. 6.6- and 19.9-GHz methanol emission towards 353.410-0.360

also have the masers projected against centimetre radio continuum (Argon et al. 2000; Kawamura & Masson 1998) and associated 6035-MHz OH masers Baudry et al. (1997). We have examined the literature to look at the association with radio continuum and OH maser transitions for all 25 sources that show 107.0-GHz methanol masers, the results are summarised in Table 3. This shows that there is a very good correlation between centimetre radio continuum and 6035-MHz OH masers and 19.9-GHz methanol masers. Most of the 19.9-GHz detections (7 of 9) are also associated with 1720-MHz OH maser emission, which is only detected in about 7% of OH maser sources in star forming regions (Caswell 1998). There is only one source (323.740-0.263) which lacks both radio continuum emission and 6035-MHz OH masers and has 19.9-GHz methanol and the weak, broad nature of the emission in this source means that it may be thermal. Further, there is also only one source (35.201-1.736/W48) which has the class II methanol masers projected against radio continuum emission, has associated 6035-MHz OH masers but does not show 19.9-GHz methanol emission. However, the absolute position of the class II methanol masers with respect to the radio continuum emission has not been accurately determined in this source and so it may not be a true exception. As all the sources in our sample are 107.0-GHz methanol masers further observations are required to determine if 19.9-GHz methanol masers are found more generally towards sources projected against centimetre radio continuum with 6035-MHz OH masers. We can use the observed association between 19.9-GHz methanol, 6035-MHz OH and radio continuum and the Cragg et al. (2002) model of methanol and OH masers to constrain the conditions in these sources.

4.2 Maser Modelling

The methanol maser model of Sobolev & Deguchi (1994) can account for maser action in the 19.9-GHz $2_1 - 3_0$ E transition, as well as in the other 8 class II maser transitions for which observations are listed in Table 4 (Sobolev et al. 1997). The same model has been applied to OH masers in star-forming regions (Cragg et al. 2002). When both molecules are highly abundant in the gas phase, masers of methanol and OH can be excited under the same model conditions, consistent with the close associations which are often observed. Here we examine model predictions in relation to the newly identified trends for sources exhibiting 19.9-GHz methanol maser emission.

In the model of Sobolev & Deguchi, the maser pumping is produced by infrared emission from warm dust at temperatures exceeding 100 K. For methanol this is sufficient to pump the molecules to their second torsionally excited state; for OH the pumping proceeds via excited rotational states. The maser pumping is strongest when the gas is significantly cooler than the dust, although some masers persist even when the gas and dust temperatures are comparable. The masers are thermally quenched at gas densities exceed-

Table 3. The association of 107.0-GHz methanol masers with centimetre radio continuum emission (are the class II masers projected against the radio continuum) and OH masers. References : 1=Argon et al. (2000); 2=Baudry et al. (1997); 3=Caswell (1998); 4=Caswell (2003); 5=Caswell (2004); 6=Caswell & Haynes (1983); 7=Dickel et al. (1982); 8=Dodson & Ellingsen (2002); 9=Ellingsen et al. (1996); 10=Forster & Caswell (2000); 11=Gaume & Mutel (1987); 12=Kawamura & Masson (1998); 13=Minier et al. (2000); 14=Onello et al. (1994); 15=Phillips et al. (1998); 16=Szymczak, Kus & Hrynek (2000); 17=Walsh et al. (1998)

Name		**Associated with**		**References**
	cm continuum	**19.9 GHz methanol**	**OH maser transitions**	
W3(OH)	Y	Y	1612,1665,1667,1720,4765,6030,6035	2,11,12,16
188.946+0.886	N	N	1665	1
192.600–0.048	N	N		13
310.144+0.760		N	1665,1667	3
318.948–0.196	N	N	1665,1667	3,9
323.740–0.263	N	Y	1665,1667	3,15
327.120+0.511	Y	N	1665,1667	3,15
328.808+0.633	Y	Y	1665,1667,1720,4765,6030,6035	3,4,5,8,17
336.018–0.827		N	1665,1667	3
339.884–1.259	Y	Y	1665,1667,1720,6030,6035	3,4,5,9
340.054–0.244	N	N	1665,1667	3,17
340.785–0.096	N	N	1665,1667,1720,6035	3,4,5,17
345.003–0.223	Y	Y	1665,1667,1720,6030,6035	3,4,5,17
345.010+1.792	Y	Y	1665,1667,6030,6035	3,4,17
345.504+0.348	N	N	1665,1667	3,17
348.703–1.043	N	N	1665	3,17
NGC6334F	Y	Y	1665,1667,1720,6030,6035	3,4,5,9
353.410–0.360	Y	Y	1665,1720,4765,6030,6035	3,4,5,8,15
9.621+0.196	Y	N	1665,1667	3,15
12.909–0.260	N	N	1665,1667,1720	3,5,17
23.010–0.411	N	N	1665,1667	6,10
23.440–0.182	N	N	1665,1667	6,10
35.201–1.736	Y	N	1665,1667,6035	4,6,14
Cep A		N	1665,1667,4765,6030,6035	1,2,16
NGC7538	Y	Y	1665,1667,1720,4765,6035	1,2,7,16

ing 10^9 cm^{-3}. Very large column densities of methanol and OH are required to account for observed maser brightness temperatures, which can be as great as 10^{12} K. For plausible maser dimensions, this implies large abundances relative to hydrogen (e.g. $X_{\rm M} = 10^{-6}$, $X_{\rm OH} = 5 \times 10^{-8}$), which are believed to follow from the evaporation of icy grain mantles in the neighbourhood of a young stellar object (Hartquist et al. 1995). In the model calculations, the maser intensities can be enhanced by beaming, and by the amplification of continuum radiation from an underlying ucH II region. The principal parameters governing the behaviour of the masers are the dust temperature $T_{\rm d}$ which drives the maser pumping, the gas kinetic temperature $T_{\rm k}$ and hydrogen density $n_{\rm H}$ which influence the collisional relaxation, and the beaming factor ϵ^{-1} and specific column density $N/\Delta V$ of methanol or OH which determine the optical depth. In terms of these parameters the column density of the species in question along the line of sight is given by $\epsilon^{-1} \times N/\Delta V \times \Delta V$, where ΔV is the velocity width of the maser line.

One of the major sources of uncertainty in excitation studies of methanol has been the influence of collisions, which has until now been modelled on propensity rules derived from a small number of experiments (Lees & Haque 1974). State-to-state rate coefficients for rotational excitation of methanol have recently been calculated (Pottage, Flower & Davis 2002, 2004), and here we report the first methanol maser calculations to employ the new data. We include collisional transitions between the methanol torsional ground state levels, assuming the collision partners to be 20% He and 80% para-H_2 (rate coefficients involving ortho-H_2 are not yet available). Data are provided for methanol energy levels up to J=9, so we extrapolated these to higher J values using the $1/\Delta$J propensity rule. A full investigation of the effects of the improved collision modelling on the masers, and of the minor effects of collisions involving higher torsional states, will be published elsewhere.

The masers are sensitive to the model conditions, switching on and off as parameters representing physical conditions are varied, with different combinations of maser lines appearing in different regimes. The masers at assorted frequencies which are observed in a given source often appear at the same velocity, and we assume this to mean that they are simultaneously excited. In this case, the model can be used to identify physical conditions which produce the same combination of masers. Observations at high spatial resolution are required to test this assumption by establishing whether or not the masers coincide in position.

Figures 9-12 illustrate a range of model conditions under which methanol and OH masers become active. Each plot shows the behaviour of maser brightness temperature as a single model parameter is varied. The upper panels include data for 7 of the methanol masers for which observations are collected in Table 4: 6.6, 12.1, 19.9, 23.1, 85.5, 86.6 and 107.0 GHz. Curves for 108.8 and 156.6 GHz are omitted in the interests of clarity – these resemble the curves for

107.0 GHz, but are generally weaker. The lower panels show the behaviour of the 7 most prevalent OH masers at 1612, 1665, 1667, 1720, 4765, 6030 and 6035 MHz. The strongest and most widespread observed masers (6.6-GHz methanol and 1665-MHz OH) are shown as bold traces; in most cases these are also the strongest masers in the models. The calculations were based around conditions which illustrate significant methanol maser action at 19.9 GHz: gas temperature $T_\mathrm{k} = 50$ K, dust temperature $T_\mathrm{d} = 175$ K, hydrogen density $n_\mathrm{H} = 10^7$ cm^{-3}, and methanol specific column density $N_\mathrm{M}/\Delta V = 10^{12}$ cm^{-3}s. The OH specific column density is $N_\mathrm{OH}/\Delta V = 10^{11}$ cm^{-3}s. In these calculations the beaming factor was $\epsilon^{-1} = 10$. Since 19.9-GHz emission is detected in sources where the methanol masers are projected against radio continuum emission, we also included background continuum radiation in the modelling. The H II continuum spectrum has temperature $T_\mathrm{e}[1 - \exp(-(f_\mathrm{e}/\nu)^2)]$ K, where $T_\mathrm{e} = 10^4$ K and $f_\mathrm{e} = 12$ GHz, and is geometrically diluted by a factor $W_\mathrm{HII} = 0.002$. Apart from the choice of parameter values and the new collision rate coefficients for methanol, the model calculations are identical to those described in full detail in Cragg et al. (2002).

For all but one of the sources in Table 4 the flux density at 107.0 GHz exceeds that at 19.9 GHz, the exception being the very strong 19.9-GHz maser in NGC 6334F. To compare these flux densities S with the model calculations of maser brightness temperature T_b requires an estimate of the maser source angular extent Ω, since S depends on $\nu^2 \Omega T_\mathrm{b}$. In the absence of this information, we seek models which can reproduce the observed flux density ratios, assuming that the masers of different frequency in the same source have a common size. When the frequency factor is taken into account, the observations suggest that for the sources where the 19.9-GHz emission is detected (excepting NGC6334F), the ratio of maser brightness temperatures for the component at the 19.9-GHz peak velocity lies in the range $0.07 \leq T_\mathrm{b}(19.9)/T_\mathrm{b}(107.0) \leq 17$. Thus the models which best represent the sources in our sample, all of which have detectable 107.0-GHz maser emission, will be those in which the 107.0-GHz maser is relatively strong. Conditions representing the sources with associated 19.9-GHz emission are likely to be in the vicinity of the intersection of the 19.9-GHz (dotted) and 107.0-GHz (dashed) traces. The correlation between 19.9-GHz methanol emission and 6030- and 6035-MHz OH emission in the model can be examined by comparing the dotted traces in the upper and lower panels of Figs 9-12.

Fig. 9 shows the variation with gas temperature T_k. The strongest methanol masers are, as observed, at 6.6 and 12.1 GHz, with the 19.9-GHz maser being most favoured at gas temperatures below 50 K. As the 23.1-GHz maser is also rather strong at gas temperatures up to 100 K, its nondetection (Cragg et al. 2004) can set useful limits on model parameters, but note that the 23.1-GHz survey was made with lower sensitivity than obtained in the current investigation at 19.9 GHz. Based on this plot, our observed flux density ratios would suggest that NCG 6334F may have rather low gas temperature (< 50 K, consistent with the earlier modelling of Cragg et al. 2001) , the other 19.9-GHz maser sources may have temperatures in the range $50 - 150$ K, while the sources in which no 19.9-GHz maser was detected may have temperatures in the same range or higher. Gas temperatures above 100 K in the majority of sources would be consistent with the scarcity of masers at 23.1, 85.5, 86.6, 108.8 and 156.6 GHz. Note that such one-dimensional analysis is very simplistic, since different choices of gas density, dust temperature, methanol abundance etc. will influence the conclusions drawn, but this nevertheless gives a useful starting point for future multidimensional fitting of the model to the observations. The lower panel of Fig. 9 shows that the 6030-, 6035- and 1720-MHz OH masers are also favoured by gas temperatures below 75 K, in keeping with their observed correlation with 19.9-GHz methanol masers.

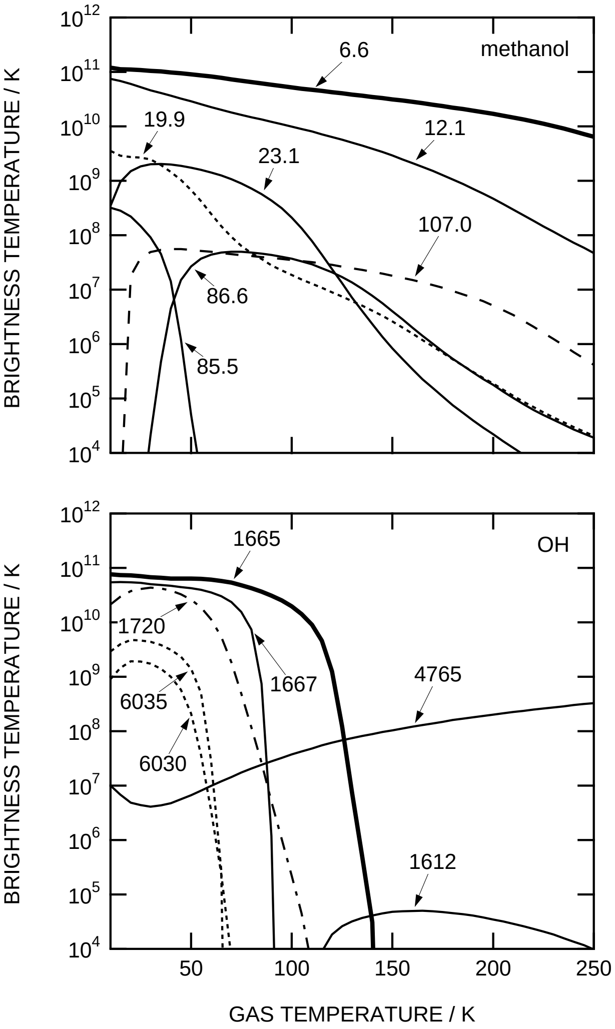

Figure 9. Variation of maser brightness temperature T_b with gas kinetic temperature T_k for models with dust temperature $T_\mathrm{d} = 175$ K and gas density $n_\mathrm{H} = 10^7$ cm^{-3}. Top panel shows behaviour of 7 methanol masers, labelled with the approximate transition frequency in GHz, with methanol specific column density $N_\mathrm{M}/\Delta V = 10^{12}$ cm^{-3}s. Bottom panel shows 7 OH masers, labelled with the approximate transition frequency in MHz, with $N_\mathrm{OH}/\Delta V = 10^{11}$ cm^{-3}s.

Fig. 10 shows the variation with dust temperature T_d. The 19.9-GHz maser is strongest for dust temperatures $100 - 200$ K. This is consistent with the infrared observations of De Buizer et al. (2000, 2002) which suggest dust temperatures in the range $120 - 160$ K for our 19.9-GHz

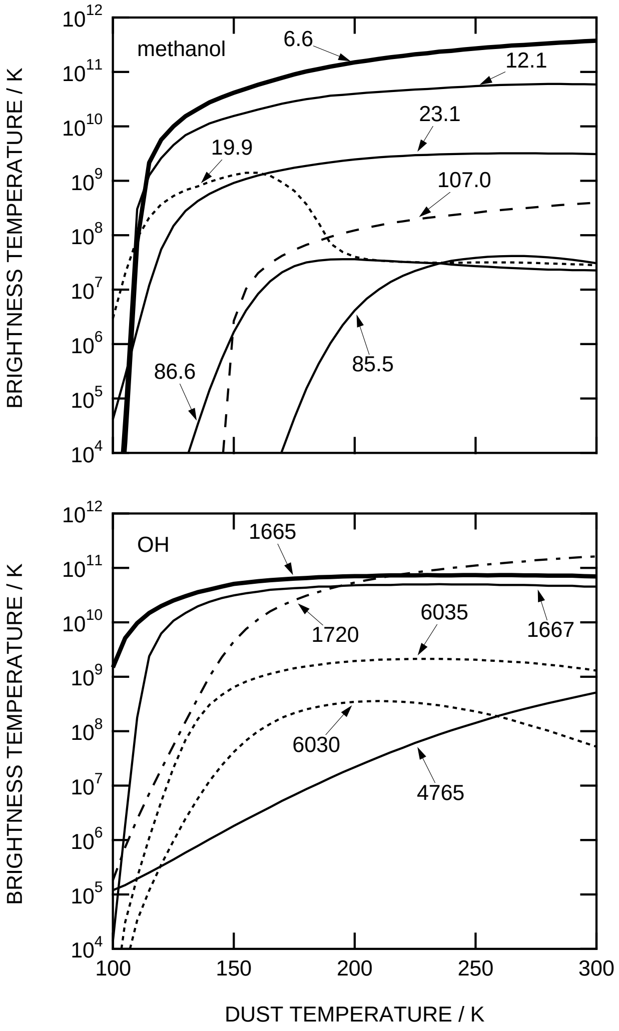

Figure 10. Variation of maser brightness temperature T_{b} with dust temperature T_{d} for models with gas kinetic temperature $T_{\mathrm{k}} = 50$ K and gas density $n_{\mathrm{H}} = 10^{7}\ \mathrm{cm}^{-3}$. Top panel shows behaviour of 7 methanol masers, labelled with the approximate transition frequency in GHz, with methanol specific column density $N_{\mathrm{M}}/\Delta V = 10^{12}\ \mathrm{cm}^{-3}\mathrm{s}$. Bottom panel shows 7 OH masers, labelled with the approximate transition frequency in MHz, with $N_{\mathrm{OH}}/\Delta V = 10^{11}\ \mathrm{cm}^{-3}\mathrm{s}$.

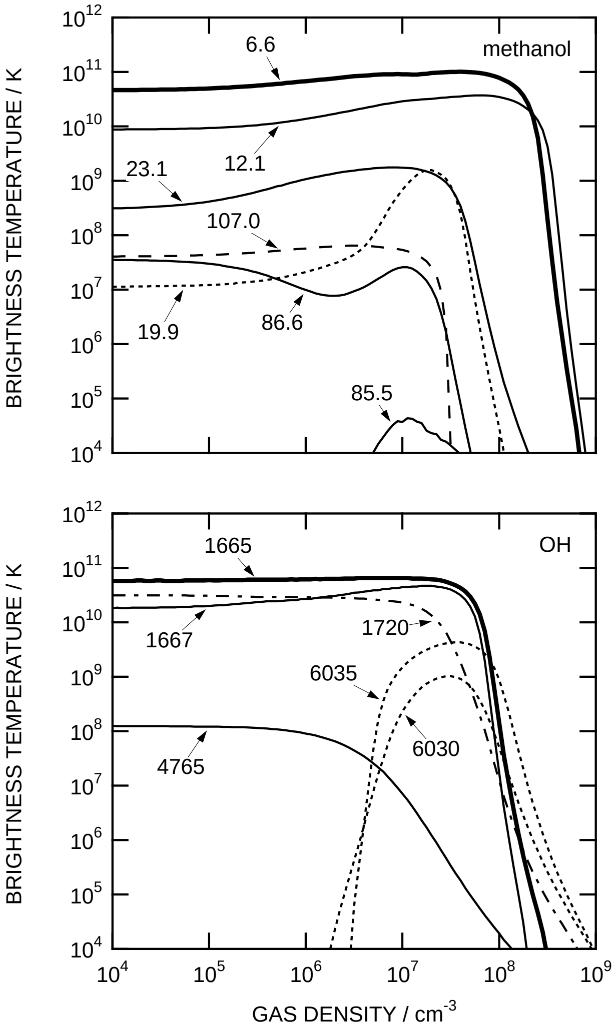

Figure 11. Variation of maser brightness temperature T_{b} with gas density n_{H} for models with gas temperature $T_{\mathrm{k}} = 50$ K and dust temperature $T_{\mathrm{d}} = 175$ K. Top panel shows behaviour of 7 methanol masers, labelled with the approximate transition frequency in GHz, with methanol specific column density $N_{\mathrm{M}}/\Delta V = 10^{12}\ \mathrm{cm}^{-3}\mathrm{s}$. Bottom panel shows 7 OH masers, labelled with the approximate transition frequency in MHz, with $N_{\mathrm{OH}}/\Delta V = 10^{11}\ \mathrm{cm}^{-3}\mathrm{s}$.

methanol maser sources, as noted in section 3.1. The various transitions have slightly different threshold temperatures for maser activity. For example the 107.0-GHz methanol maser requires dust temperature above 150 K to turn on under the chosen conditions, and is brighter than the 19.9-GHz maser at temperatures above 200 K. The 6030-, 6035- and 1720-MHz OH masers are also strong at dust temperatures above 150 K.

Fig. 11 shows the variation with gas density n_{H}. All the masers are thermally quenched at the highest density $10^{9}\ \mathrm{cm}^{-3}$. Under the conditions illustrated the 107.0-GHz maser is quenched at $n_{\mathrm{H}} > 10^{7.5}\ \mathrm{cm}^{-3}$, while the 19.9-GHz line is strongest for densities $10^{6.5} - 10^{8}\ \mathrm{cm}^{-3}$. These conditions also favour maser activity in the 6030-, 6035- and 1720-MHz OH transitions.

Fig. 12 shows the variation with specific column density $N/\Delta V$ of methanol and OH. The calculations on which Figs 9-11 are based have $N_{\mathrm{M}}/\Delta V = 10 \times N_{\mathrm{OH}}/\Delta V$, following Cragg et al. (2002) where it was established that this factor accounts well for the observed intensity ratios of the dominant 6.6-GHz methanol and 1665-MHz OH masers. Fig. 12 shows that this factor also provides substantial common ground between the 19.9-GHz methanol and 6030-, 6035- and 1720-MHz OH masers, in keeping with the correlation identified by our observations. The plotted brightness temperatures suggest that our sample of 107.0-GHz methanol maser sources have $N_{\mathrm{M}}/\Delta V$ in the range $10^{11} - 10^{12.5}\ \mathrm{cm}^{-3}\mathrm{s}$.

We may conclude that the maser models are able to account qualitatively for the detection of 19.9-GHz methanol masers in 9 out of 25 of the 107.0-GHz sources, and are also able to explain the correlation found between methanol

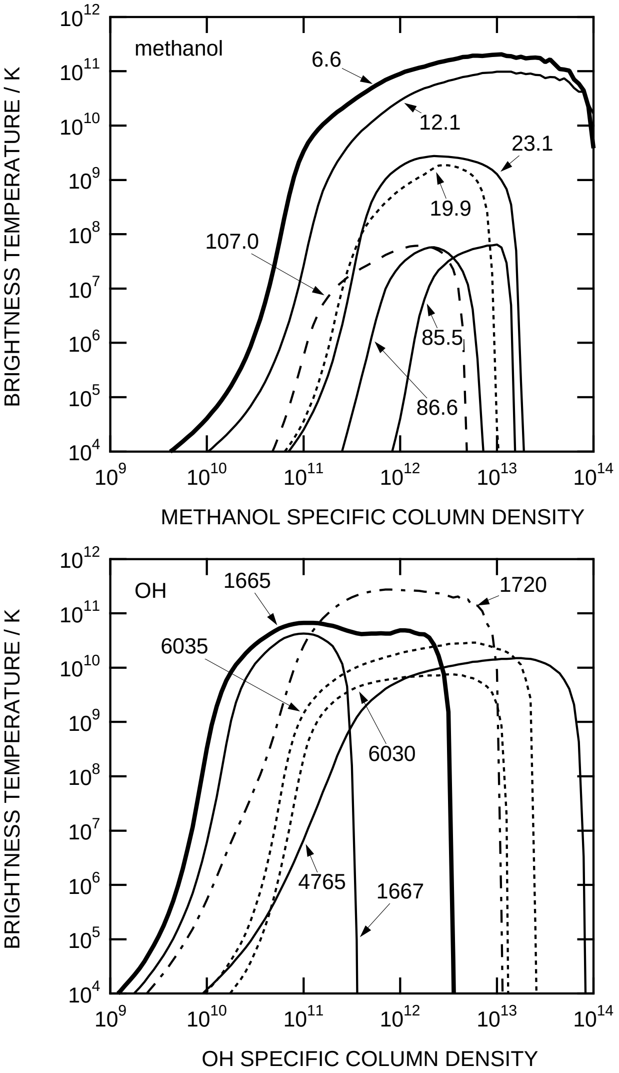

Figure 12. Variation of maser brightness temperature T_b with specific column density of methanol or OH. Models have gas kinetic temperature $T_\mathrm{k} = 50$ K, dust temperature $T_\mathrm{d} = 175$ K and gas density $n_\mathrm{H} = 10^7$ cm^{-3}. Top panel shows behaviour of 7 methanol masers, labelled with the approximate transition frequency in GHz, while bottom panel shows 7 OH masers, labelled with the approximate transition frequency in MHz.

emission at 19.9 GHz and OH masers at 6035 MHz. The model calculations suggest that the 19.9-GHz maser sources have gas temperatures around 50 K, dust temperatures 150-200 K, gas density $10^{6.5} - 10^{7.5}$ cm^{-3}and methanol specific column density $10^{11} - 10^{12.5}$ cm^{-3}s, while the sources with no 19.9-GHz maser detected may be higher in gas or dust temperature or lower in gas density. As these estimates were determined in a simplistic fashion by varying only one model parameter at a time, they cannot be considered definitive. A more quantitative comparison between model calculations and observations in individual sources can further constrain the physical conditions which give rise to the observed masers. This is best undertaken after observations at high spatial resolution have clarified the associations between the different masers. The exceptional sources W3(OH), 345.010+1.792 and NGC6334F have been the subject of previous detailed modelling of this type (Sutton et al. 2001; Cragg et al. 2001), and fitting of the maser model to observations of the 25 107.0-GHz maser sources is the subject of ongoing work. For this purpose further model calculations are required to explore the multidimensional parameter space in the regions identified above.

5 CONCLUSIONS

We have made the first sensitive search for the 19.9-GHz transition of methanol in the southern hemisphere and detected 6 new sources, taking the total number to 9. There is a strong correlation between sources which show 19.9-GHz methanol emission and those which both have the class II methanol masers projected against radio continuum and have associated 6035-MHz OH. This suggests that the 19.9-GHz methanol masers trace a narrow range of physical conditions, probably associated with a specific evolutionary phase. We have made a preliminary examination of this association in the model of Cragg et al. (2002) and find it to be consistent with a gas temperatures of 50 K, dust temperatures of 150-200 K and gas densities of $10^{6.5} - 10^{7.5}$ cm^{-3}, although further modelling is required to more thoroughly sample the parameter space.

ACKNOWLEDGEMENTS

This research has made use of NASA's Astrophysics Data System Abstract Service. This research has made use of the SIMBAD database operated at CDS, Strasbourg, France. The authors thank David Flower for making methanol rate coefficient data available prior to publication. Financial support for this work was provided by the Australian Research Council. AMS was supported by the Ministry of Industry, Science and Technology of the Russian Federation (Contract No. 40.022.1.1.1102).

REFERENCES

Argon, A. L., Reid, M. J., Menten, K. M. 2000, ApJS 129, 159

Batrla, W., Matthews, H. E., Menten, K. M., Walmsley, C. M. 1987, Nat 326, 49

Baudry, A., Desmurs, J. F., Wilson, T. L., Cohen, R. J. 1997, A&A 325, 255

Caswell, J. L. 1998, MNRAS 297, 215

Caswell, J. L. 2003, MNRAS 341, 551

Caswell, J. L. 2004, MNRAS in press

Caswell, J. L., Haynes, R. F. 1983, Aust. J. Phys. 36, 417

Caswell, J. L., Vaile, R. A., Ellingsen, S. P., Whiteoak, J. B., Norris, R. P. 1995a, MNRAS 272, 96

Caswell, J. L., Vaile, R. A., Ellingsen, S. P., Norris, R. P. 1995b, MNRAS 274, 1126

Caswell, J. L., Yi, J., Booth, R. S., Cragg, D. M. 2000, MNRAS 313, 599

Cesaroni, R., Walmsley, C. M. 1991, A&A 241, 537

Cragg, D. M., Sobolev, A. M., Ellingsen, S. P., Caswell, J. L., Godfrey, P. D., Salii, S. V., Dodson, R. G. 2001, MNRAS 323, 939

Cragg, D. M., Sobolev, A. M., Godfrey, P. D. 2002, MNRAS 331, 521

Cragg, D. M., Sobolev, A. M., Caswell, J. L., Ellingsen, S. P., Godfrey, P. D. 2004, MNRAS in press

De Buizer, J. M., Piña, R. K., Telesco, C. M. 2000, ApJSS 130, 437

De Buizer, J. M., Walsh, A. J., Piña, R. K., Phillips, C. J., Telesco, C. M. 2002, ApJ 564, 327

Dickel, H. R., Rots, A. H., Goss, W. M., Forster, J. R. 1982, MNRAS 198, 265

Dodson, R. G., Ellingsen, S. P. 2002, MNRAS 333, 307

Ellingsen, S. P., Norris, R. P., McCulloch, P. M. 1996, MNRAS 279, 101

Ellingsen, S. P., Cragg, D. M., Minier, V., Muller, E., Godfrey, P. D. 2003, MNRAS 344, 73

Forster, J. R., Caswell, J. L. 2000, ApJ 530, 371

Gaume, R. A., Mutel, R. L. 1987, ApJS 65, 193

Gray, M. D., Field, D., Doel, R. C. 1992, MNRAS 262, 555

Hartquist T. W., Menten K. M., Lepp S., Dalgarno, A. 1995, MNRAS 272, 184

Kawamura, J. H., Masson, C. R. 1998, ApJ 509, 270

Koo, B., Williams, D. R. W., Heiles, C., Backer, D. C. 1988, ApJ 326, 931

Lees, R. M., Haque, S. S. 1974, Can J Phys 52, 2250

Mehringer, D. M., Zhou, S., Dickel, H. R. 1997, ApJ 475, L57

Mehrotra S. C., Dreizler H., Mäder H. 1985, Z. Naturforsch 40a, 683

Menten, K. M. 1991a, in ASP Conf. Ser. 16, Atoms, ions and molecules: New results in spectral line astrophysics, ed. A. D. Haschick & P. T. P. Ho, 119

Menten, K. M. 1991b, ApJ 380, L75

Menten, K. M., Johnston, K. J., Wadiak, E. J., Walmsley, C. M., Wilson, T. L. 1988, ApJ 331, L41

Menten, K. M., Batrla, W. 1989, ApJ 341, 839

Menten, K. M., Reid, M. J., Pratap, P., Moran, J. M., Wilson, T. L. 1992, ApJ 401, L39

Minier, V., Booth, R. S., Conway, J. E. 2000, A&A 362, 1093

Minier, V., Booth, R. S. 2002, A&A 387, 179

Minier, V., Ellingsen, S. P., Norris, R. P., Booth, R. S. 2003 A&A 403, 1095

Norris, R. P., Whiteoak, J. B., Caswell, J. L., Wieringa, M. H., Gough, R. G. 1993, ApJ 412, 222

Onello, J. S., Phillips, J. A., Bengalia, P. 1994, ApJ 426, 249

Pavlakis, K. G., Kylafis, N. D. 1996a, ApJ 467, 300

Pavlakis, K. G., Kylafis, N. D. 1996b, ApJ 467, 309

Phillips, C. J. 1998, PhD Thesis, University of Tasmania

Phillips, C. J., Norris, R. P., Ellingsen, S. P., McCulloch, P. M. 1998, MNRAS 300, 1131

Pottage, J. T., Flower, D. R., Davis, S. L. 2002, J. Phys. B 35, 2541

Pottage, J. T., Flower, D. R., Davis, S. L. 2004, MNRAS in press

Slysh, V. I., Kalenskii, S. V., Val'tts, I. E. 1995, ApJ 442, 668

Sobolev A.M., Deguchi S., 1994, A&A, 291, 569

Sobolev A.M., Cragg D.M., Godfrey P.D., 1997, MNRAS, 288, L39

Sutton, E. C., Sobolev, A. J., Ellingsen, S. P., Cragg, D. M., Mehringer, D. M., Ostrovskii, A. B., Godfrey, P. D. 2001, ApJ 554, 173

Szymczak, M., Hrynek, G., Kus, A. J. 2000, A&ASS 143, 269

Szymczak, M., Kus, A. J., Hrynek, G. 2000, MNRAS 312, 211

Val'tts, I. E. 1998, Astron. Lett 24, 788

Val'tts, I. E., Dzura, A. M., Kalenskii, S. V., Slysh, V. I., Booth, R. S., Winnberg, A. 1995, A&A 294, 825

Val'tts, I. E., Ellingsen, S. P., Slysh, V. I., Kalenskii, S. V., Otrupcek, R., Voronkov, M. A. 1999, MNRAS 310, 1077

Walsh, A. J., Hyland, A. R., Robinson, G., Burton, M. G. 1997, MNRAS 291, 261

Walsh, A. J., Burton, M. G., Hyland, A. R., Robinson, G. 1998, MNRAS 301, 640

Walsh, A. J., Lee, J. -K., Burton, M. G. 2002, MNRAS 329, 475

Wilson, T. L., Walmsley, C. M., Snyder, L. E., Jewell, P. R. 1984, A&A 134, L7

Wilson, T. L., Walmsley, C. M., Menten, K. M., Hermsen, W. 1985, A&A 147, L19

arXiv:astro-ph/0407246v1 13 Jul 2004

Table 1. The flux density at the velocity of the peak in the 19.9-GHz transition, (or the 107.0-GHz transition for sources with no 19.9-GHz emission) of the 86.6-, 107.0-, 108.8- & 156.6-GHz methanol transitions towards all star formation regions with known 107.0-GHz methanol masers. The 19.9-GHz data is where indicated by a †. The 6.6-GHz data for the seven Tidbinbilla 19.9-GHz detections are taken from this work except for 339.884-1.259 and the 12.1 328.808+0.633 and 339.884-1.259 are taken from this work. The rest of the information has been taken from the literature references given in the last are quoted they are 3 times the RMS noise level in the spectra. Transitions where thermal emission is detected are indicated with a * and the upper flux density of the thermal emission at the listed velocity. References : 1=Batrla et al. (1987); 2=Caswell et al. (1995a); 3=Caswell et al. (1995b); 4=C et al. (2001); 6=Cragg et al. (2004); 7=Ellingsen et al. (2003); 8=Koo et al. (1988); 9=Mehringer, Zhou & Dickel (1997); 10=Menten (1991b); 11=Minier (1998); 13=Slysh, Kalenskii & Val'tts (1995); 14=Sutton et al. (2001); 15=Szymczak, Hrynek & Kus (2000); 16=Val'tts et al. (1995); 17=Val'tts et al. (1 19=Wilson et al. (1984); 20=Wilson et al. (1985)

		Flux Density								
Source	**Velocity (km s^{-1})**	**6.6-GHz (Jy)**	**12.1-GHz (Jy)**	**19.9-GHz (Jy)**	**23.1-GHz (Jy)**	**85.5-GHz (Jy)**	**86.6-GHz (Jy)**	**107.0-GHz (Jy)**	**108.8-GHz (Jy)**	**156.**
W3(OH)	-43.3	3000	600	44.3†	9.5	<0.7	6.7	72	<0.6	
188.946+0.886	10.9	495	235	<0.20		<2.1	<0.8	15.5	<4.8	
192.600-0.048	4.2	72	<0.4	<0.19		<1.8	<2.2	5.8	<4.5	
310.144+0.760	-56	130	114	<0.16	<0.8	<1.4	<2.1	23		
318.948–0.196	-34.2	780	180	<0.17	<0.8	<2.0	<2.2	5.7	< 3*	
323.740–0.263	-51.4	132	135	0.15	<0.9	<1.8	<1.9	9.5	<5.4	
327.120+0.511	-89.8	25	5	<0.17	<0.9	<1.5	<2.2	9.2		
328.808+0.633	-43.7	315	5	0.8	<1.0	1.6	<2.4	5.5	< 6*	
336.018–0.827	-40	40	25	<0.21	<0.8	<1.3	< 2.7	6	<5.7	
339.884–1.259	-36.2	300	213	9.8	<0.6	<1.1	< 1.7	30	<5.4	
340.054–0.244	-62.8	0.3	<1	<0.20	<0.8		<2.3	2.9		
340.785–0.096	-105.9	144	43	<0.76	<0.7	<1.8	<1.9	6.1		
345.003–0.223	-27.4	27	<0.5	0.22	<0.6	<2.0	<2.9	2	< 1.5*	
345.010+1.792	-17.6	120	2	0.21	<0.5	<2.8	<2.6	4	<5	
345.504+0.348	-17.7	174	4.7	<0.65	<0.8	<4.7	<2.4	2.3	< 2*	
348.703–1.043	-3.3	60	34.5	<0.39	<0.9	<1.5	<2.7	7.6		
NGC6334F	-10.4	2530	1100	147	32.8	< 2.5*	< 1.0*	14.8		
353.410–0.360	-20.5	40	8	0.33	<0.8	<2.1	<2.0	4.5		
9.621+0.196	-0.5	100	10	<0.22	<0.6	<1.5	<2.3	22	< 3*	
12.909–0.260	39.5	317	11.5	<0.27	<0.8	<3.8	<8.6	5.5	< 3*	
23.010–0.411	75.9	405	28	<0.26	<0.9	<3.8		5.2	<5.1	
23.440–0.182	97.2	23	9	<0.24	<0.9	< 4.0*	<4.1	4.4		
35.201–1.736	42	560	25	<0.51	<0.9	<1.1	<2.3	24	<4.8	
Cep A	-2.2	1420	<7			<5.0	<5.0	16	<5.0	
NGC7538	-59.0	15	<5	0.21†	0.21	<5.0	<5.0	10.1	< 4.0*	